Ultrasound-guided injections of ultrasound contrast agents and *p53* gene for the treatment of rat with breast cancer.

Yonggang Dai[1], Xiaoguang Wang[2], Hongxia Hu[3]*

[1]Clinical Laboratory, Shandong Provincial Third Hospital, PR China

[2]Central Hospital of Liaocheng, Liaocheng, Shandong, PR China

[3]The 2nd Department of Urology, Gansu Provincial Hospital, PR China

Abstract

Objective: This study aimed to explore ultrasound-guided injections of Ultrasound Contrast Agents (UCAs) and *p53* gene for the treatment of rats with breast cancer.

Methods: With the construction of *p53* expression vector and rat model with breast cancer, 160 rats that modeled successfully were randomly divided into 4 groups: *p53* gene introduction group, *p53* gene introduction+ultrasound irradiation group, *p53* gene introduction+CUAs group and *p53* gene introduction+CUAs+ultrasound irradiation group. With regular ultrasonography after *p53* injection, the rats were killed after 14 d, and the tumors were separated and weighed to calculate the tumor inhibition rate. H and E staining was used to observe the tumor tissues. The expression of *p53* in tumor tissues was detected by Quantitative Real-Time Polymerase Chain Reaction (qRT-PCR), Western blotting and immunohistochemically staining, respectively.

Results: In the *p53* gene introduction and *p53* gene introduction+CUAs groups, the tumor volume of rats significantly increased, with uneven echoes and abundant blood-flow signals, the tumor cells with good growth and acidophilic cytoplasm, and *p53* had low expression. In the *p53* gene introduction +ultrasound irradiation group, the tumor volume of rats increased slowly, surrounded by blood-flow signals and necrotic tumor tissues, with a tumor inhibition rate of 36.30%, and the expression of *p53* was higher than that in the *p53* gene introduction and *p53* gene introduction+CUAs groups. In the *p53* gene introduction+CUAs+ultrasound irradiation group, the tumor volume of rats increased slightly, blood-flow signals significantly decreased, the tumor cells had extensive degeneration and necrosis with a tumor inhibition rate of 62.62%, and the expression of *p53* was higher than that in other three groups.

Conclusion: Ultrasound irradiation after ultrasound-guided injections of UCAs and *p53* gene could increase the expression of *p53* gene, thus inhibit the growth of rat with breast cancer.

Introduction

Breast cancer is the most common malignancy and the leading cause of cancer deaths among females [1]. It has been reported that 1.7 million women are diagnosed with breast cancer each year, causing 520,000 deaths worldwide. In addition, breast cancer accounts for 25% of all cancer cases and 15% of all cancer deaths in women [2,3]. Although a lot of risk factors such as hormonal, environmental and lifestyle factors have been found, the etiology of breast cancer is not clearly known. Furthermore, some molecular markers have been identified to be correlated with the risk of this disease [4]. Many improved technologies and adjuvant therapies have contributed to remarkable decrease in incidence and mortality of breast cancer, and detection at an early stage significantly increases the five-year survival rate of over 90% breast cancer patients. Despite great scientific improvements and main clinical advancements, the patients with malignant breast cancer still have a poor prognosis [5,6]. Therefore, it is essential to find efficient targeted therapies for the treatment of breast cancer.

Ultrasound Contrast Agents (UCAs) are gas-filled, encapsulated microbubbles that can be injected into the bloodstream typically ranging from 1 to 10 μm in diameter [7,8]. When insolated, these microbubbles have stable oscillation to produce broadband signals at harmonic frequencies and at resonance, causing the microbubbles to fragment and subsequent inertial collapse [9,10]. Nonlinear oscillations of UCAs generate a subharmonic of the incident ultrasound and enhance the ultrasound signals as well as the

signal-to-noise ratio. Furthermore, UCAs may release the encapsulated gas with acoustic forcing *via* sufficiently high-pressure amplitude, resulting in subharmonic backscatter because of subsequent oscillations [11,12]. *P53* is a key tumor suppressor gene as the guardian of the genome that is inactivated by somatic mutations in approximately 50% of human cancers [13]. As a transcription factor, *p53* is identified to be the first member of the *p53* family, eliciting genome maintenance by regulating cell cycle arrest, DNA repair, senescence and apoptosis in response to a broad range of cellular stresses [14]. It has been reported that the survival of tumor cells lacking functional *p53* is increased due to the decreased apoptosis ability of cells [15]. So far, gene therapy with wild-type *p53* and UCAs has been observed to be effective for the treatment of some cancers [16]. The purpose of this study is to explore ultrasound-guided injections of ultrasound contrast agents and *p53* gene for the treatment of rat with breast cancer.

Materials and Methods

Ethic statement

All experiments conformed to the standard of Animal Ethics of our hospital (The First Affiliated Hospital of Xinjiang Medical University, Urumqi, Xinjiang, China).

Study subjects and grouping

A total of 200 male Wistar rats (weighing 170~300 g) were fed at 12 h interval and the maintained room temperature and humility were 20°C and 50%, respectively. All rats were obtained from the Animal center of our hospital. If there is any rat died during the experiment, new rat was collected follow the principle of random sampling method and treated with relevant process.

Construction of p53 eukaryotic expression vector

BamH I (D1010A, Takara Biotechnology Ltd., Dalian, China) and EcoR I (D3320, Takara Biotechnology Ltd., Dalian, China) double enzyme plasmid pGEX-*p53* (included wild type *p53* cDNA sequence) and pcDNA3.1$^+$ (Invitrogen Inc., Carlsbad, CA, USA) underwent 1.5% agarose gel electrophoresis, after which DNA purification kits was applied to collect the target fragment (TIANGEN Biotech Co., Ltd., Beijing, China). Then, the target fragment was connected by T4 ligase (D2011A, Takara Biotechnology Ltd., Dalian, China), after which samples were transformed into the Escherichia coli DH5α competent cell and cultured in plate containing penbritin at 37°C overnight. On the next day, monoclonal colony was selected for enlarged culture and a small part of the cells were used to produce plasmid DNA. Double enzyme digestion of BamH I and EcoR I was performed to testify whether the recombinant clone was a success or not, and the primers of T7 and BGH promoter were applied for the sequencing analysis on both sides.

Construction of rat model with breast cancer and gene introduction

Awake 256 tumor line of breast cancer (Shanghai Institute of Pharmaceutical Industry, Shanghai, China) was inoculated into the enterocoelia of 4 w old Wistar rats. One week later, malignant ascites was extracted and trypan blue (T6146, Sigma-Aldrich Chemical Company, St Louis MO, USA) was used to dye cells. Cells number was calculated under microscope and the concentration of cells was adjusted to 1×10^8/ml. Cell suspension (0.2 ml, 2×10^7 cells) was inoculated into 200 Wistar rats from pectoral fascia to construct breast cancer rat model. Ten days after inoculation, high-resolution ultrasound was performed to testify the maximum Length (L), Width (W) and Thickness (T) of tumor. *p53* gene introduction was conducted on rats with the tumor diameter of 2.0~2.5 cm. The method for *p53* gene introduction: 200 μl UCAs microbubble was obtained using microsyringe (fluorocarbon, presented by Nanfang hospital, southern medical university), mixed with 4 μg *p53* eukaryotic expression plasmid and kept at 4°C for 30 min. *p53* gene was attached to the albumin shell of UCAs microbubble, after which 200 μl UCAs and (or) 4 μg *p53* eukaryotic expression plasmid were injected into the central area of tumor of each rat.

Animal grouping

Rats (n=160) with the tumor diameter of 2.0~2.5 cm were subcutaneously injected with *p53* gene under ultrasonic guidance and randomly assigned into 4 groups (n=40): the group injected with 4 μg *p53* gene only, the group with 4 μg *p53* gene injection combined with ultrasound irradiation (4C1 probe, emission frequency: 1.75 MHz, received frequency: 3.5 MHz, mechanical index: 1.0, irradiation time: 5 min and focusing depth: 3 cm), the group injected with 4 μg *p53* gene and 200 μl UCAs microbubble without ultrasound irradiation and the group injected with 4 μg *p53* gene and 200 μl UCAs microbubble under ultrasound irradiation (4C1 probe, emission frequency: 1.75 MHz, received frequency: 3.5 MHz, mechanical index: 1.0, irradiation time: 5 min and focusing depth: 3 cm).

Tumor volume and tumor inhibition rate

After the gene introduction, tumor size, internal echo, blood flow, maximum Length (L), Width (W) and Thickness (T) of tumor were detected every week to calculate the tumor volume (Tumor volume cm^3=1/2 (L × W × T)). After 14 d of gene introduction, rats in all the groups were put to death. Tumor was removed and weighed to calculate the tumor inhibition rate. The tumor inhibition rate (%)=(1-average weight of tumor in the experiment group/average weight of tumor in the control group) × 100%. A group was regarded as the control group and the rest three groups were regarded as the experiment group.

H and E staining

Fresh rat tissues were stored in 10% formalin for 24 h fixation and made into 4 μm paraffin sections after ethanol dehydrating,

transparentizing, dewaxing and embedding. After conventional dewaxing, sections received hematoxylin staining (5 min) and were washed up by water. After hydrochloric acid (1%) alcohol differentiation and ammonia water washing, sections were re-dyed by eosin for 3 min and were washed up by water. Gradient ethanol dehydration and xylene transparency twice for 10 min were conducted. Then, the remaining xylenes around the sections were erased, after which neutral balsam was quickly added and cover glass was used to seal the sections. The double-blind method: histological changes of rat kidney tissues were observed under light microscope. Xylene, ethyl alcohol, hematoxylin, eosin and neutral balsam were purchased from Sigma-Aldrich Chemical Company (St Louis MO, USA). LM1235 paraffin slicing machine was obtained from (Leica Microsystem, Germany). KD-BM paraffin embedding machine was purchased from (Jinhua Kennono Electronic Technology Co., Ltd, Zhejiang, China). Biologic photomicroscope CX-31 was from Olympus Optical Co., Ltd (Tokyo, Japan).

Quantitative real-time polymerase chain reaction (qRT-PCR)

Tumor tissues of rats were obtained and Trizol (15586-026, Invitrogen Inc., Carlsbad, CA, USA) was applied to extract the total RNA. RNA (500 ng) was collected for reverse transcription which was performed in accordance with the specification of Reverse Transcription System A3500 kit (A3500, Promega Corp., Madison, Wisconsin, USA). According to the gene sequences published by GenBank, the Primer 5.0 was used to design the primer, which was produced by Shanghai Sangon Biological Engineering Technology & Services Co., Ltd. (Shanghai, China). Reaction condition of SYBR Green: predenaturation at 95°C for 15 min with one cycle; at 95°C for 30 s, at 56°C for 30 s, and at 72°C for 90 s, 40 cycles. Reaction system: 12.5 μl Premix Ex Taq or SYBR Green Mix, 1 μl Forward Primer, 1 μl Reverse Primer, 1-4 μl DNA template, ddH2O up to 25 μl. β-actin was used as the internal reference gene and the standard of control group was set as 1 to calculate the C_t value of target gene. Relative Quantification (RQ)=$2^{-\Delta\Delta Ct}$. The RQ value was used for statistical analysis. The real-time fluorescent quantitative PCR (iQ5) was purchased from Bio-Rad Laboratories (Hercules, CA, USA).

Western blotting

The proteins in the tumor tissues of rats were extracted and detected by the bicinchoninic acid (BCA) kit (P0012, Beyotime Biotechnology Co., Shanghai, China) to detect the concentration of proteins. Protein, added with 5X loading buffer (Beyotime Biotechnology Co., Shanghai, China) was boiled at 95°C for 10 min. Each well contained 30 μg samples which were electrophoretic separated by 10% polyacrylamide. Polyvinylidene Fluoride (PVDF) was used to transfer the membrane, after which samples were sealed by 5% Bovine Serum Albumin (BSA) at room temperature for 1 h. Tris Buffered Saline with Tween (TBST) diluted primary antibody

β-actin (ab8226, 1: 1000; Abcam Inc., Cambridge, MA, USA) and *p53* (ab1431, 1 μg/ml) were added at 4°C overnight. TBST was used to wash membrane 3 times and relevant secondary antibody was added for reaction at 37°C for 2 h (Abcam Inc., Cambridge, MA, USA). Chromophore-labeled substrate A and B solution (Promega Corporation, Madison, WI, USA) were 1: 1 mixed for developing at room temperature for 1 min, after which samples were wrapped by plastic wrap and transferred into the dark room. The exposed X-ray image was developed and photographic fixing was conducted. Gel-Pro analyzer 4.0 was applied for band analysis. The protein expression was reflected by the ratio of the grey value of target protein and grey value of β-actin. The decolorizing shaking table (ZD-9500) was purchased from HLD Corporation, Taicang, Jiangsu, China and vertical electrophoresis tank was obtained from Bio-Rad, Inc. (Hercules, CA, USA).

Immunohistochemical staining

After dewaxing and hydration, the tumor tissue sections of rats were boiled (15 min) in citrate buffer solution (pH=6.0) for antigen retrieval. Then, endogenous peroxidase was inactivated and the primary and secondary antibody of *p53* were added (Abcam Inc., Cambridge, MA, USA). Diaminobenzidine (DAB) staining, hematoxylin re-dyeing and dehydration of gradient ethanol were performed, after which sections were sealed in neutral balsam. The Phosphate Buffer Saline (PBS) solution was added in the control experiment to replace the primary antibody. Brown particle in colloid or nucleus was observed in positive cells under light microscope. The percentage of the positive cells in the total cells was regarded as the analysis index. One out of three sections was selected and 10 visual fields were randomly obtained on each section to calculate the average value. Power Vision immunohistochemical detection system, PBS solution, citrate buffer solution (pH=6.0) and DAB kit were purchased from Beijing Zhongshan Jinqiao Biotechnology Co., Ltd. (Beijing, China).
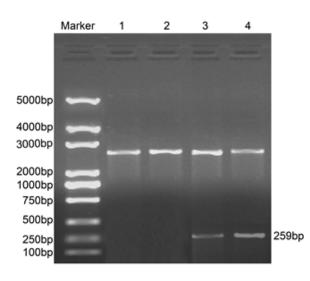
Statistical analysis

Data were analysed using the Statistical Package for the Social Sciences (SPSS) version 21.0 (SPSS Inc.; Chicago, IL, USA). Continuous data were displayed as mean ± Standard Deviation (SD) (x̄ ± s) and the normality and homogeneity of variance test were applied for the ratio of groups. The differences between two groups were analysed by Least Significant Difference (LSD)-t test and One-Way Analysis of Variance (ANOVA) was conducted for comparisons among more than two groups. $P<0.05$ was regarded as statistically significant different.

Results

Construction of p53 eukaryotic expression vector

BamH I and EcoR I dual-enzyme were applied to digest *p53* eukaryotic expression vector. Agarose gel electrophoresis was performed and clear band was observed at 259 bp. The length
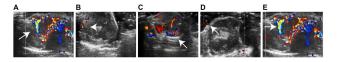
of inserted target gene accorded with the estimated length (Figure 1).

Figure 1. BamH I and EcoR I double enzyme digestion pf p53 eukaryotic expression plasmid Notes: M: Marker; 1 and 2: empty plasmid; 3 and 4: p53 eukaryotic expression plasmid.

Ultrasonic observation of rat tumor after p53 gene introduction

The tumor volume of the *p53* gene introduction group increased as time went on and the morphology was irregular with uneven internal echo and rich blood flow signal. In the *p53* gene introduction+ultrasound irradiation group, the tumor volume increased slowly with uneven internal echo and detectable blood signals. Hypoecho was noted in the *p53* gene introduction+CUAs group. Slight increase of tumor volume and significant decrease of blood signal were observed in the tumor of the *p53* gene introduction+CUAs+ultrasound irradiation group (Figure 2).
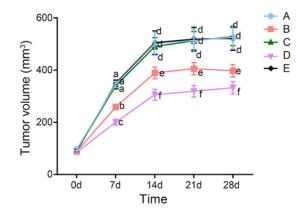

Figure 2. Ultrasound figures of rat tumor with different way of p53 gene introduction. Notes: A group: p53 gene introduction group; B group, p53 gene introduction+ultrasound irradiation group; C group, p53 gene introduction+CUAs group; D group, p53 gene introduction +CUAs+ultrasound irradiation group.
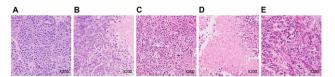
Changes of tumor volume and tumor inhibition rate after p53 gene introduction

The tumor in the *p53* gene introduction and *p53* gene introduction+CUAs groups kept sustainable growth and the tumor volume significantly increased. The tumor inhibition rate of the *p53* gene introduction+CUAs group was 3.72%. Compared with the *p53* gene introduction and *p53* gene introduction+CUAs groups, the tumor of the *p53* gene introduction+ultrasound irradiation group grew slowly and the tumor inhibition rate was 36.30% (P=0.017). The tumor
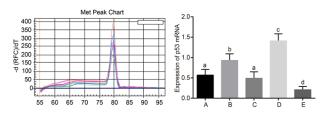
volume of the *p53* gene introduction+CUAs+ultrasound irradiation group slightly increased and the tumor inhibition rate was 62.62%, which was significantly higher than that of the *p53* gene introduction+ultrasound irradiation group (P=0.027) (Figure 3).

Figure 3. Comparison of tumor volume before and after p53 gene introduction in rats of each group. Notes: A group: p53 gene introduction group; B group, p53 gene introduction+ultrasound irradiation group; C group, p53 gene introduction+CUAs group; D group, p53 gene introduction+CUAs+ultrasound irradiation group; different letter represents significant difference at the level of 5%.

Figure 4. H and E staining of rat tumor after p53 gene introduction in rats of each group. Notes: A group: p53 gene introduction group; B group, p53 gene introduction+ultrasound irradiation group; C group, p53 gene introduction+CUAs group; D group, p53 gene introduction +CUAs+ultrasound irradiation group.

Figure 5. p53 expression in tumor tissues detected by qRT-PCR. Notes: Left figure, the p53 mRNA solubility curve; right figure, expressions of p53 mRNA in tumor tissues of rats; A group: p53 gene introduction group; B group, p53 gene introduction+ultrasound irradiation group; C group, p53 gene introduction+CUAs group; D gr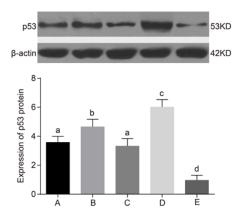oup, p53 gene introduction+CUAs+ultrasound irradiation group; different letter represents significant difference at the level of 5%.

H and E staining after p53 gene introduction

Cells in the *p53* gene introduction and *p53* gene introduction +CUAs groups were in the shape of polygon and grew well; the cell nucleus was big and deeply dyed; the cytoplasm showed acidophil. In the *p53* gene introduction+ultrasound irradiation group, necrotic tissue and residual carcinoma tissue

were observed in the tumor tissues of rats. As for the *p53* gene introduction+CUAs+ultrasound irradiation group, the tumor cells of rat showed degeneration necrosis in large area and the structure was vague; karyopyknosis, karyorrhexis and apoptosis body were noted (Figure 4).

Figure 6. p53 protein expressions in tumor tissues of rats in each group detected by Western blotting. Notes: Upper figure, Western blotting for the p53 protein expressions of rats in each group; Lower figure, expressions of p53 protein in tumor tissues of rats in each group; A group: p53 gene introduction group; B group, p53 gene introduction+ultrasound irradiation group; C group, p53 gene introduction+CUAs group; D group, p53 gene introduction+CUAs +ultrasound irradiation group; different letter represents significant difference at the level of 5%.
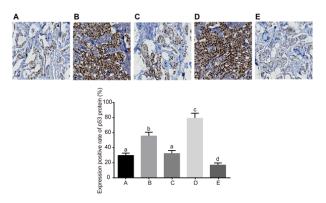

Figure 7. Expressions of p53 in tumor tissue of rats in each group detected by immunohistochemically staining. Notes: Upper figure, expressions of p53 protein in tumor tissues of rats in each group detected by immunohistochemically staining; Lower figure, positive expression rate (%) of p53 protein in tumor tissues of rats; A group: p53 gene introduction group; B group, p53 gene introduction +ultrasound irradiation group; C group, p53 gene introduction CUAs group; D group, p53 gene introduction+CUAs+ultrasound irradiation group; different letter represents significant difference at the level of 5%.

Expression of p53 in tumor tissues of rats

No significant difference was found between the *p53* gene introduction and *p53* gene introduction+CUAs groups (P=0.103). Compared with the *p53* gene introduction and *p53* gene introduction+CUAs groups, the mRNA and protein expressions of *p53* significantly increased in the *p53* gene

introduction+ultrasound irradiation group (P=0.021). The *p53* gene introduction+CUAs+ultrasound irradiation group showed the highest mRNA and protein expressions of *p53* in tumor tissues of rats as compared with the other three groups (Figures 5-7).

Discussion

Recently, contrast-enhanced ultrasound of clinical applications has become widespread to promote the ability of collecting microvascular and vascular information in various tumors, including breast cancer, lung cancer, gastric cancer, etc. [17-20]. In this study, we aim to explore the effects of combined UCAs and *p53* gene on the development and progression of breast cancer. And we demonstrate that ultrasound irradiation following combined injection of UCAs and *p53* gene enhances exogenous *p53* expression in breast cancer, thus inhibiting tumor growth of breast cancer in rat model.

Initially, we find that in the *p53* gene introduction and *p53* gene introduction+CUAs groups, the tumor volume is significantly increased with inhomogeneous echoes and abundant blood flow signals. Additionally, the tumor cells exhibit an ideal growing status with acidophilic cytoplasm and lower *p53* expression. Yet, when after the ultrasound irradiation is performed in the *p53* gene introduction+CUAs group, the *p53* expression increases slightly. In the *p53* gene introduction+CUAs+ultrasound irradiation group, the level of *p53* reaches the highest, together with the optimal inhibitory efficacy on the tumor growth among the 4 groups. *p53* is considered as a critical tumor suppressor and is comprised of two domains, a C terminal oligomerization domain and a core DNA-Binding domain [21]. The wild-type *p53* is closely connected with cell-cycle arrest, apoptosis, and DNA sequence reparation [22]. And loss of *p53* gene can result in human cancers [23], because mutant *p53* can lead to abnormal mitoses and induce cell apoptosis. Mutant *p53* can also promote proliferation, invasion and cell survival as its oncogenic properties [24]. Honda and his colleagues reported that the transcriptional effects of exogenous *p53* gene can be promoted by an upstream estrogen response element, leading to lower transfection rates through inhibition on the cell cycle [25]. The experiment of Liu et al. also confirmed that exogenous *p53* played an important role in improving cell death in Hepatocellular Carcinomas (HCC), therefore enhancing therapeutic effects in HCC patients who lack normal *p53* functions [26]. It is also demonstrated by He et al. that targeted delivery of exogenous *p53* gene induces in tumor cells a *p53*-dependent anti-proliferative reaction, which can be an effective approach for cancer treatment [27].

The *p53* gene introduction+CUAs group is treated with ultrasound irradiation, and apart from increased *p53* level, this group displays alleviated tumor growth speed hereafter, and the blood signal is only detected in peripheral area. Tumor tissues demonstrate necrosis and the antitumor rate are elevated compared with the *p53* gene introduction and *p53* gene introduction+CUAs groups. In comparison with the *p53* gene

introduction+CUAs group, the *p53* gene introduction+CUAs +ultrasound irradiation group showed increased *p53* expression and a slight increase of tumor size and lessened blood signal. The tumor tissues demonstrate extensive necrosis and degeneration. Contrast-enhanced ultrasound is a powerful tool to monitor antiangiogenic ability in cancer [28]. Ultrasound has been largely applied for targeted and noninvasive medical therapies owing to its ability to penetrate tissue with less amelioration of energy, and in terms of gene therapy, it has been utilized to enhance the ability of naked DNA to enter mammalian cells [29]. UCA is an excellent carrier of genes, which can be crushed by ultrasound irradiation, thus releasing high concentrations of genes and significantly increasing permeability of cell membranes of local capillaries and adjacent tissues, making it easier for foreign genes to enter into the capillaries, into the tissues, and then into the cells and enhancing gene transfection, gene expression and the gene effect in the targeted region [30]. The experiment of Qi et al. suggests the similar result that ultrasonic irradiation may improve the gene transfection and expression efficiency of interventional adenovirus-*p53* in liver cancer treatment [31]. Those changes in the *p53* gene introduction+CUAs+ultrasound irradiation group suggest that the exogenous *p53* gene is carried by the CUAs, which is destroyed by the operation of ultrasonic irradiation, thus facilitating *p53* gene enters the targeted area to serve its inhibitory function on tumor growth.

Thus, our study provide evidence that with assistance of ultrasound irradiation, combined injection of CUAs and *p53* gene elevated exogenous *p53* expression in breast cancer, which exerts inhibitory effects on tumor growth of breast cancer in rat model. Furthermore, our findings may provide novel understandings for management of breast cancer.

References

1. Mai K, Makoto N, Tsuyoshi N, Toshiaki I, Takanobu S, Hiroyuki U, Kenichi S. Clinicopathological relevance of kinesin family member 18A expression in invasive breast cancer. Oncol Lett 2016; 12: 1909-1914.

2. Zafrakas M, Papasozomenou P, Emmanouilides C. Sorafenib in breast cancer treatment: A systematic review and overview of clinical trials. World J Clin Oncol 2016; 7: 331.

3. Gouri A, Dekaken A, El Bairi K, Aissaoui A, Laabed N, Chefrour M, Ciccolini J, Milano G, Benharkat S. Plasminogen activator system and breast cancer: potential role in therapy decision making and precision medicine. Biomarker Insights 2016; 11: 105.

4. Tazzite A, Kassogue Y, Diakite B, Jouhadi H, Dehbi H, Benider A, Nadifi S. Association between ABCB1 C3435T polymorphism and breast cancer risk: a Moroccan case-control study and meta-analysis. BMC Gene 2016; 17: 126.

5. van Reesema LL, Zheleva V, Winston JS, Jansen RJ, OConnor CF, Isbell AJ, Bian M, Qin R, Bassett PT, Hinson VJ, Dorsch KA. SIAH and EGFR, two RAS pathway biomarkers, are highly prognostic in locally advanced and metastatic breast cancer. E Biomedicine 2016; 11: 183-198.

6. Fiskaa T, Knutsen E, Nikolaisen MA, Jørgensen TE, Johansen SD, Perander M, Seternes OM. Distinct small RNA signatures in extracellular vesicles derived from breast cancer cell lines. PloS One 2016; 11: 0161824.

7. King D, OBrien W. Correspondence: Quantitative analysis of ultrasound contrast agent postexcitation collapse. IEEE Transactions on Ultrasonics, Ferroelectrics, and Frequency Control 2014; 61: 1237-1241.

8. Gruber MJ, Bader KB, Holland CK. Cavitation thresholds of contrast agents in an in vitro human clot model exposed to 120 kHz ultrasound. J Acoust Soc Am 2014; 135: 646-653.

9. Liberman A, Wang J, Lu N, Viveros RD, Allen CA, Mattrey RF, Blair SL, Trogler WC, Kim MJ, Kummel AC. Mechanically tunable hollow silica ultrathin nanoshells for ultrasound contrast agents. Adv Funct Mater 2015; 25: 4049-4057.

10. Xu S, Hu H, Jiang H, Xu ZA, Wan M. Ultrafast 2-dimensional image monitoring and array-based passive cavitation detection for ultrasound contrast agent destruction in a variably sized region. J Ultras Med 2014; 33: 1957-1970.

11. Koppolu S, Chitnis PV, Mamou J, Allen JS, Ketterling JA. Correlation of rupture dynamics to the nonlinear backscatter response from polymer-shelled ultrasound contrast agents. IEEE Transactions on Ultrasonics, Ferroelectrics, and Frequency Control 2015; 62: 494-501.

12. Appis AW, Tracy MJ, Feinstein SB. Update on the safety and efficacy of commercial ultrasound contrast agents in cardiac applications. Echo Res Pract 2015; 2: 55-62.

13. Luo H, Cowen L, Yu G, Jiang W, Tang Y. SMG7 is a critical regulator of p53 stability and function in DNA damage stress response. Cell Discov 2016; 2: 15042.

14. Ren X, Liu H, Zhang M, Wang M, Ma S. Co-expression of ING4 and P53 enhances hypopharyngeal cancer chemosensitivity to cisplatin in vivo. Mol Med Rep 2016; 14: 2431-2438.

15. An Y, Liu T, He J, Wu H, Chen R, Liu Y, Wu Y, Bai Y, Guo X, Zheng Q, Liu C. Recombinant Newcastle disease virus expressing P53 demonstrates promising antitumor efficiency in hepatoma model. J Biomed Sci 2016; 23: 55.

16. Ren X, Liu H, Zhang M, Wang M, Ma S. Co-expression of ING4 and P53 enhances hypopharyngeal cancer chemosensitivity to cisplatin in vivo. Mol Med Rep 2016; 14: 2431-2438.

17. Saracco A, Szabo BK, Tanczos E, Bergh J, Hatschek T. Contrast-enhanced ultrasound (CEUS) in assessing early response among patients with invasive breast cancer undergoing neoadjuvant chemotherapy. Acta Radiologica 2017; 58: 394-402.

18. Wang S, Yang W, Fu JJ, Sun Y, Zhang H, Bai J, Chen MH, Yan K. Microflow imaging of contrast-enhanced ultrasound for evaluation of neovascularization in peripheral lung cancer. Medicine 2016; 95.

19. Lang SA, Moser C, Gehmert S, Pfister K, Hackl C, Schnitzbauer AA, Stroszczynski C, Schlitt HJ, Geissler EK,

Jung EM. Contrast-enhanced ultrasound (CEUS) detects effects of vascular disrupting therapy in an experimental model of gastric cancer. Clin Hemorheol Microcirc 2014; 56: 287-299.

20. Dong Y, Zhang XL, Mao F, Huang BJ, Si Q, Wang WP. Contrast-enhanced ultrasound features of histologically proven small (≤ 20 mm) liver metastases. Scand J Gastroenterol 2017; 52: 23-28.

21. Liu DP, Song H, Xu Y. A common gain of function of p53 cancer mutants in inducing genetic instability. Oncogene 2010; 29: 949.

22. Riley T, Sontag E, Chen P, Levine A. Transcriptional control of human p53-regulated genes. Nat Rev Mol Cell Biol 2008; 9: 402.

23. Liu X, Wilcken R, Joerger AC, Chuckowree IS, Amin J, Spencer J, Fersht AR. Small molecule induced reactivation of mutant p53 in cancer cells. Nucl Acids Res 2013; 41: 6034-6044.

24. Muller PA, Vousden KH. p53 mutations in cancer. Nat Cell Biol 2013; 15: 2.

25. Honda KI, Kajitani K, Nobeyama H, Kira Y, Yabunaka Y, Egami M, Zhi X, Fukuda T, Yoshida H, Matsumoto Y, Ichimura T. An upstream estrogen response element linked to exogenous p53 tumor suppressor gene expression differentiates effects of the codon 72 polymorphism. Asian Pac J Cancer Prev 2011; 12: 865-868.

26. Liu X, Wang S, Guo X, Wei F, Yin J, Zang Y, Li N, Chen D. Exogenous p53 and ASPP2 expression enhances rAdV-TK/GCV-induced death in hepatocellular carcinoma cells lacking functional p53. Oncotarget 2016; 7: 18896.

27. He Y, Nie Y, Xie L, Song H, Gu Z. p53 mediated apoptosis by reduction sensitive shielding ternary complexes based on disulfide linked PEI ternary complexes. Biomater 2014; 35: 1657-1666.

28. Hoyt K, Warram JM, Umphrey H, Belt L, Lockhart ME, Robbin ML, Zinn KR. Determination of breast cancer response to bevacizumab therapy using contrast-enhanced ultrasound and artificial neural networks. J Ultras Med 2010; 29: 577-585.

29. Ninomiya K, Yamada R, Meisaku H, Shimizu N. Effect of ultrasound irradiation on bacterial internalization and bacteria-mediated gene transfer to cancer cells. Ultras Sonochem 2014; 21: 1187-1193.

30. Li XH, Zhou P, Wang LH, Tian SM, Qian Y, Chen LR, Zhang P. The targeted gene (KDRP-CD/TK) therapy of breast cancer mediated by SonoVue and ultrasound irradiation in vitro. Ultrasonics 2012; 52: 186-191.

31. Qi JS, Wang WH, Li FQ. Combination of interventional adenovirus-p53 introduction and ultrasonic irradiation in the treatment of liver cancer. Oncol Lett 2015; 9: 1297-1302.

*Correspondence to

Correspondence to

Hongxia Hu

The 2nd Department of Urology

Gansu provincial hospital

PR China